

Microscopic identification of native donor Ga-vacancy complexes in Te-doped GaAs

J. Gebauer* and M. Lausmann

Fachbereich Physik, Martin-Luther-Universität Halle-Wittenberg, D-06099 Halle, Germany

T. E. M. Staab

*Fachbereich Physik, Martin-Luther-Universität Halle-Wittenberg, D-06099 Halle, Germany
and Laboratory of Physics, Helsinki University of Technology, P.O. Box 1100, FIN-02015 HUT, Finland*

R. Krause-Rehberg

Fachbereich Physik, Martin-Luther-Universität Halle-Wittenberg, D-06099 Halle, Germany

M. Hakala and M. J. Puska

Laboratory of Physics, Helsinki University of Technology, P.O. Box 1100, FIN-02015 HUT, Finland

(Received 31 August 1998; revised manuscript received 30 November 1998)

Native vacancies in Te-doped (5×10^{16} – 5×10^{18} cm $^{-3}$) GaAs were investigated by means of positron lifetime and Doppler-broadening coincidence spectroscopy. The experimental data were related to theoretical calculations of the positron lifetime and the annihilation momentum distribution. Monovacancies were observed in all Te-doped GaAs samples under study. It will be shown that they can directly be identified to be Ga-vacancy–Te_{As}-donor complexes. These complexes are the dominating type of vacancy defects in the doping range under observation. [S0163-1829(99)07327-0]

Vacancies may determine important properties of semiconductor materials like GaAs. They mediate, e.g., dopant diffusion¹ or reduce the density of free carriers.^{2,3} The detailed microscopic identification of vacancies and vacancy complexes in GaAs was, however, found to be difficult. Most theoretical calculations^{4,5} as well as diffusion studies¹ indicate a dominating role of negative Ga vacancies in *n*-doped GaAs. In contrast, a recent calculation showed that also the As vacancy could be an abundant defect in highly *n*-doped GaAs due to a low formation energy.⁶ Moreover, pairing of acceptorlike vacancies with positive donors is expected due to Coulomb attraction. Evidence for such complexes is based on photoluminescence,⁷ infrared absorption,² and theoretical considerations of the doping behavior.³ Recently, scanning tunneling microscopy (STM) directly identified Si_{Ga}-donor–Ga-vacancy complexes on cleavage planes of highly Si-doped GaAs (Ref. 8) later shown to be present with the same density in the bulk.⁹ To our knowledge no such direct identification has been obtained so far for other *n* dopants, e.g., tellurium. Positron annihilation, however, is directly sensitive to vacancies. Positron lifetime spectroscopy indeed showed the existence of native vacancies in *n*-doped GaAs.^{10–12} However, the positron lifetime measurement (which probes mainly the open volume) is not alone able to identify the defects as a given isolated arsenic¹⁰ or gallium¹¹ vacancy, or as a vacancy-impurity complex.¹²

One possibility to overcome the difficulty mentioned above is the investigation of the positron annihilation momentum distribution. The high momentum part of this distribution can be used to identify the chemical surrounding of the annihilation site.^{13–16} This is based on the fact that tightly bound core electrons with high momenta retain their element-specific properties even in a solid. This allows the identification of vacancies and vacancy-impurity complexes, especially when measurements are correlated to calculations

of the momentum distribution.¹³ The coincident detection of both 511-keV γ quanta from single annihilation events allows the observation of the high momentum annihilation distribution due to a strong reduction of the disturbing background.^{13–16} Ga vacancies in highly Si-doped GaAs were identified using that Doppler-broadening coincidence technique.¹⁷ The experiment could, however, not decide whether the vacancies are isolated or a part of a complex because the Si_{Ga} donor on the second nearest site is not expected to contribute much to the annihilation.¹⁷ Thus, the identification of dopant-vacancy complexes in GaAs by positron annihilation is still an open question.

Tellurium is incorporated in the As sublattice only.³ If pairing with neighboring Ga vacancies occurs, a measurable contribution to the annihilation is expected, i.e., an identification of this complex could be possible. However, the momentum distribution for the vacancy cannot be undoubtedly determined when the fraction of trapped positrons (η) is unknown. Therefore we use correlated positron lifetime measurements to obtain η .¹⁴ The experimental results are compared with theoretical calculations of the annihilation characteristics to obtain a safe interpretation.

The samples studied were cut from Te-doped GaAs crystals grown by the liquid encapsulated Czochralski technique. The carrier concentration was $n = 5 \times 10^{16}$, 5×10^{17} , 1.5×10^{18} , and 5×10^{18} cm $^{-3}$. The crystals were investigated as-received as well as annealed at 1100 °C under high (5.6 bar) arsenic pressure. The annealing conditions were chosen to maintain arsenic-rich stoichiometry and result in a maximum vacancy density for a given crystal.¹⁸ The material with $n = 5 \times 10^{16}$ cm $^{-3}$ was not annealed. Highly Si-doped GaAs ([Si] = 1×10^{19} and 4×10^{19} cm $^{-3}$) was investigated for comparison since V_{Ga}-Si_{Ga} complexes were identified by STM in samples from the same wafers.⁹ Positron lifetime spectroscopy was performed using a conventional system (time reso-

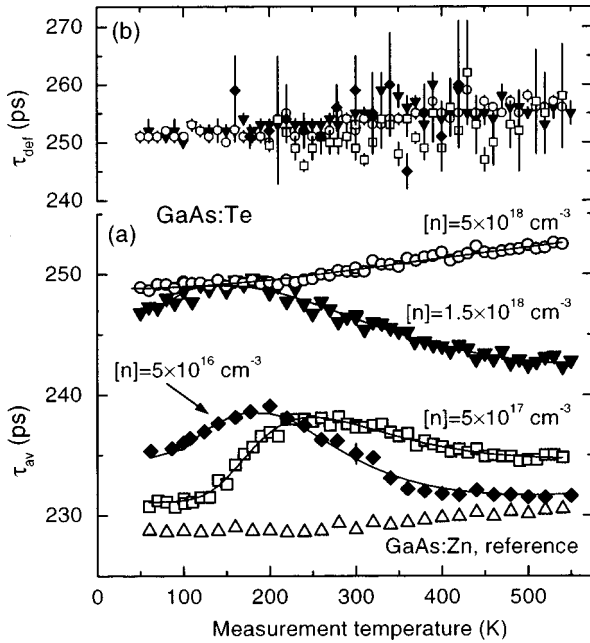


FIG. 1. Average positron lifetime τ_{av} (a) and defect-related lifetime τ_{def} (b) vs measurement temperature in Te-doped GaAs compared to a GaAs:Zn reference. Some samples were annealed (2 - and $5 \times 10^{18} \text{ cm}^{-3}$ at 1100°C for 1 h, $5 \times 10^{17} \text{ cm}^{-3}$ at 1100°C for 24 h) under 5.6 bar As-vapor pressure. The other samples are as received. Spectra decomposition was not reliable for $T > 350 \text{ K}$ for the $5 \times 10^{16} \text{ cm}^{-3}$ doped sample (τ_{av} is close to τ_b). Lines are fits according to the trapping model (see text).

lution 250 ps). The spectra were analyzed with the positron trapping model after source and background corrections. The annihilation momentum distribution was observed by coincidence spectroscopy at 300 K using two Ge- γ detectors in collinear geometry.¹⁵ The intensity of the core annihilation was characterized by the line-shape parameter W , defined as the integrated intensity in the region $(15-20) \times 10^{-3} m_0c$ divided by the total. Measured W parameters are normalized to the value $W = 0.0074$ of a Zn-doped GaAs reference showing no positron trapping at vacancies.

First, the positron lifetime was measured as a function of temperature (Fig. 1). About $4-5 \times 10^6$ counts were collected in each spectrum. The average positron lifetime (τ_{av}) in the GaAs:Zn reference increases slightly with temperature. This is typical for annihilation in the defect-free bulk and can be attributed to thermal lattice expansion.¹⁹ The lifetime of (229 ± 1) ps at 300 K agrees with previous results for the bulk lifetime (τ_b) in GaAs.^{10,12,19} τ_{av} in the Te-doped samples is above τ_b , indicating positron trapping at vacancies. The temperature dependence of τ_{av} in GaAs:Te is typical when positrons are trapped at negatively charged vacancies and ions. The ions (with a lifetime close to τ_b) trap positrons in their shallow potential only at low temperature. Negative ions are attributed to intrinsic defects (e.g., $\text{Ga}_{\text{As}}^{2-}$)¹⁹ or extrinsic impurities,⁹ however, positron annihilation alone does not allow their detailed identification. With increasing temperature positrons are detrapped from the ions and a larger fraction annihilate at vacancies, causing the increase of τ_{av} between 100 and 200 K. The decrease of τ_{av} at $T > 200 \text{ K}$ in the medium doped samples indicates positron trapping at negative vacancies, trapping at neutral vacancies

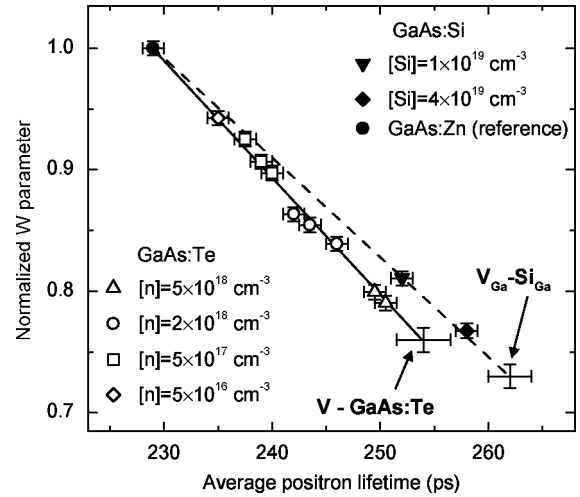


FIG. 2. Normalized W parameter vs average positron lifetime in differently Te- and Si-doped GaAs measured at 300 K. Lines are linear fits to the respective data. The annihilation parameters are indicated for the vacancies in GaAs:Te ($W = 0.76$, $\tau = 254 \text{ ps}$) and for $V_{\text{Ga}}\text{-Si}_{\text{Ga}}$ complexes in GaAs:Si ($W = 0.73$, $\tau = 262 \text{ ps}$) according to the trapping model.

would be independent of temperature.²⁰ We fitted the data considering positron trapping and detrapping at the shallow Rydberg states around ions and vacancies as well as the $T^{-1/2}$ dependence for positron trapping at negatively charged defects.^{19,20} A good agreement to the data is obtained [lines in Fig. 1(a)]. The parameters describing the temperature dependence of positron trapping are similar in all samples, e.g., the binding energy of positrons to the Rydberg states was $E_b = (65 \pm 20) \text{ meV}$ as was found earlier,^{9,19} only the concentrations of the ions and vacancies relative to each other change. Note that the decrease of τ_{av} with decreasing T in the highest doped sample can be similarly described (only E_b was fixed in the fit). Positron trapping at vacancies is practically saturated here. Thus, τ_{av} reflects the slight decrease of the defect-related lifetime, τ_d with temperature [Fig. 1(b)]. This might be attributed to lattice expansion too, although the effect is larger than in the reference. The important result for this study is that $\tau_d = (254 \pm 3) \text{ ps}$ at 300 K is the same in all samples and exhibit the same temperature dependence. This points towards a similar nature of the vacancies, assigned to be monovacancies due to the lifetime of 254 ps.⁹⁻¹²

We then have to answer the question whether the vacancies observed in GaAs:Te do indeed all have the same microscopic structure. This can be achieved by checking the linearity between τ_{av} and W parameter. The fraction of positrons annihilating in vacancies is given by $\eta = (W_b - W) / (W_b - W_d) = (\tau_{av} - \tau_b) / (\tau_d - \tau_b)$. Thus, the measured W depends linearly on τ_{av} if the defect density changes (i.e., η) and not the defect type (i.e., τ_d or W_d).¹⁶ The W - τ_{av} analysis is shown in Fig. 2. The data for differently doped GaAs:Te show a linear behavior (indicated by the solid line) within the errors. Thus, the vacancy type is identical in all Te-doped samples. Moreover, only one type of vacancies exists in all samples since the line runs through the bulk value ($\tau_b = 229 \text{ ps}$, $W_b = 1$).¹⁶ The presence of negative ions does not influence this result because their annihilation parameters agree with that of the bulk. The characteristic W parameter for the vacancy in GaAs:Te can be determined from τ_d

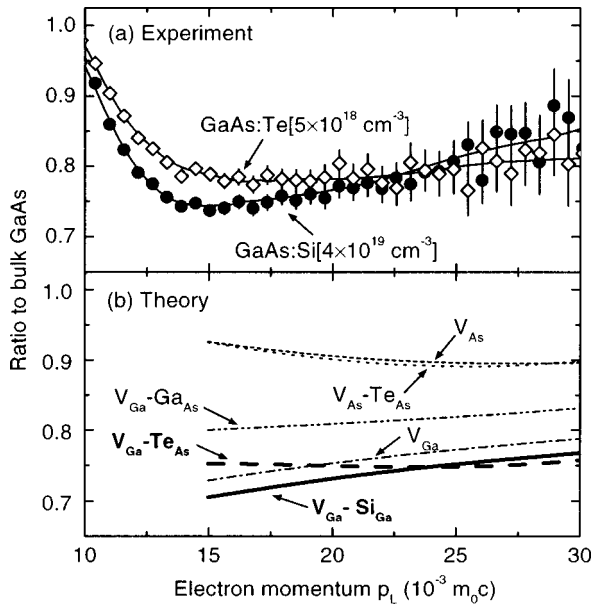


FIG. 3. (a) High momentum part of the positron annihilation momentum distribution (normalized by taking the ratio to a GaAs:Zn reference) for the vacancies in GaAs:Te and GaAs:Si. The spectra (total area 3.5×10^7 counts) were brought to unity and scaled to full trapping at the vacancies before normalization. Lines result from smoothing and serve to guide the eye only. (b) Ratio of the momentum density to bulk GaAs for different vacancies in GaAs from theoretical calculations. The curves for $V_{\text{Ga}}\text{-Te}_{\text{As}}$ and $V_{\text{Ga}}\text{-Si}_{\text{Ga}}$ complexes are highlighted to emphasize the good agreement to the respective experimental data in GaAs:Te and GaAs:Si. The theoretical curves are not accurate for $p_L < 15 \times 10^{-3} m_0c$ (Ref. 14) and hence are omitted.

$= (254 \pm 3)$ ps to be $W_d = 0.76(1)$. A similar linear variation as for GaAs:Te is found for GaAs:Si, but the slope is slightly different for the different dopants. The characteristic annihilation parameters for the $\text{Si}_{\text{Ga}}\text{-V}_{\text{Ga}}$ complexes⁹ are $\tau_d = (262 \pm 2)$ ps and $W_d = 0.73(1)$, different from the values found in GaAs:Te. This indicates a different defect type. The detailed observation of the annihilation momentum distribution shown below allows to relate the differences to the presence of a Te atom close to a Ga vacancy in GaAs:Te.

In Fig. 3(a) the high-momentum part of the annihilation momentum distribution is shown for the vacancies in GaAs:Te [$5 \times 10^{18} \text{ cm}^{-3}$] and GaAs:Si [$4 \times 10^{19} \text{ cm}^{-3}$]. The data are normalized by taking the ratio to a GaAs:Zn reference since the momentum distribution itself spans several orders of magnitude, making a detailed comparison difficult.^{15,16} The core annihilation is more intense in GaAs:Te than in GaAs:Si in the momentum range $p_L = (10 - 22.5) \times 10^{-3} m_0c$. Note that the high vacancy concentrations in our samples are necessary to obtain this result, since the high fraction ($>90\%$) of trapped positrons allows the estimation of the momentum distribution with small uncertainties. The momentum distribution at the vacancies in GaAs:Te differs also in shape, it decays steeper (or, equivalent, it is narrower) than that in GaAs:Si. This results in a crossover at $p_L \sim 22.5 \times 10^{-3} m_0c$ [Fig. 3(a)].

The observations of the momentum distribution can be explained as follows. In bulk GaAs, the dominating contribution to the core annihilation comes from Ga-3d electrons

($Z=31$).¹⁴ The As-3d electrons ($Z=33$) are more tightly bound, i.e., the momentum distribution is broader and the intensity of the core annihilation is reduced. Positron annihilation at the $\text{Si}_{\text{Ga}}\text{-V}_{\text{Ga}}$ complexes in GaAs:Si occurs mainly with 3d electrons from As. Thus, the momentum distribution should be broader compared to the bulk. This is, in fact, observed in Fig. 3(a). In contrast, at As vacancies the momentum distribution should be narrower and more intense because annihilation occurs mainly with the Ga-3d electrons.

In tellurium the main contribution to the core annihilation comes from 4d electrons that are less strongly bound than the As-3d electrons in GaAs. They contribute therefore to the core annihilation more at lower momenta and have a steeper momentum distribution. A similar difference has been noted earlier by comparing results from bulk InP, GaSb, and GaAs (Ref. 14) and for Zn-impurity P-vacancy complexes in InP.¹³ The shape of the momentum distribution measured in GaAs:Te therefore indicates that the vacancies are neighbored by Te atoms. Because Te resides on the As sublattice, the vacancy must be on the Ga sublattice. Thus we identify the vacancies in GaAs:Te to be Ga-vacancy- Te_{As} complexes. This assignment explains also the reduced positron lifetime at the vacancies in GaAs:Te since the large Te atom is expected to decrease the open volume of the neighboring Ga vacancy compared to that in the $V_{\text{Ga}}\text{-Si}_{\text{Ga}}$ complex.

To support our experimental findings, theoretical calculations of the annihilation characteristics were performed with the method introduced in Refs. 13 and 14, shown to give momentum distribution and positron lifetime in GaAs in reasonable agreement with the experiment.¹⁴ The momentum distribution is calculated within the independent particle model for each core electron state using free atomic wave functions. The final distribution is obtained by summing up the contributions from each state weighted by the partial annihilation rates calculated within the generalized gradient approximation (GGA) of positron annihilation.²¹ The GGA scheme is also used to calculate the positron lifetimes. All calculations were performed without taking lattice relaxation into account. The theoretically calculated momentum distributions for different defects and defect complexes in GaAs (normalized to the bulk distribution) are shown in Fig. 3(b), calculated positron lifetimes and W parameters are given in Table I.

The lifetime calculated for the $V_{\text{Ga}}\text{-Si}_{\text{Ga}}$ complex (267 ps) is slightly longer than experimentally observed (262 ps). However, the discrepancy is rather small and reflects the similar difference between the measured and calculated bulk lifetimes of 229 and 232 ps, respectively. Moreover, the shape of the calculated momentum distribution and hence the W parameter are in good agreement with the experimental results. Since the $V_{\text{Ga}}\text{-Si}_{\text{Ga}}$ complexes were undoubtedly identified⁹ we can use the respective data as a reference state, focusing on relative changes in the following.

The core annihilation is more intense at V_{As} than at V_{Ga} according to the calculations [Fig. 3(b)], reflected in the high calculated W parameter $W(V_{\text{As}}) = 0.91$ (Table I). This is expected from the qualitative arguments above. It should, however, be noted that the calculation overestimates the intensity of the annihilation with Ga-3d electrons, discussed in more

TABLE I. Theoretically calculated positron lifetime and W parameter (relative to the bulk) for different vacancies and vacancy complexes in GaAs.

Vacancy	τ (ps)	W_{rel}
GaAs bulk	232	1
V_{As}	266	0.92
V_{Ga}	267	0.74
$V_{\text{Ga}}\text{-Si}_{\text{Ga}}$	267	0.72
$V_{\text{Ga}}\text{-Te}_{\text{As}}$	261	0.75
$V_{\text{Ga}}\text{-Ga}_{\text{As}}$	267	0.80
$V_{\text{As}}\text{-Te}_{\text{As}}$	265	0.91
$V_{\text{As}}\text{-V}_{\text{Ga}}$	332	0.62
$V_{\text{Ga}}\text{-Te}_{\text{As}}\text{-V}_{\text{Ga}}$	272	0.67
$V_{\text{As}}\text{-V}_{\text{Ga}}\text{-Te}_{\text{As}}$	328	0.62

detail in Ref. 14. Therefore, a slightly too high W parameter may result for the As vacancy. However, the calculated positron lifetime at V_{As} (which is less influenced by the difficulties of the calculation mentioned above) is similar to that of $V_{\text{Ga}}\text{-Si}_{\text{Ga}}$ whereas τ_d measured in GaAs:Te is lower. The calculations give thus no support to identify the vacancy in GaAs:Te to be V_{As} . Similar arguments apply for the (hypothetical) $\text{Te}_{\text{As}}\text{-V}_{\text{As}}$ complex which could be formed if As vacancies were present. Divacancies or divacancy- Te_{As} complexes, on the other hand, have higher calculated positron lifetimes than $V_{\text{Ga}}\text{-Si}_{\text{Ga}}$ (Table I).

The calculated momentum distribution of isolated Ga vacancies has the same shape as the $V_{\text{Ga}}\text{-Si}_{\text{Ga}}$ complexes [Fig. 3(b)] only with slightly increased intensity. Moreover, the calculated positron lifetime of V_{Ga} agrees with that of this complex ($\tau_d \sim 267$ ps). For these reasons we exclude isolated Ga vacancies as the ones detected in GaAs:Te. It is then interesting to look for the $V_{\text{Ga}}\text{-Ga}$ -antisite complex which could, according to theory, be an abundant defect in Ga-rich, n -type GaAs.⁴ However, the shape of annihilation momentum distribution as well as the lifetime (267 ps) calculated for this defect disagrees with the experiment [Figs. 3(a) and 3(b)].

The last defect to be discussed is the $V_{\text{Ga}}\text{-Te}_{\text{As}}$ complex. The calculated lifetime for this complex (261 ps) is 6 ps lower, whereas the W parameter (0.75) is higher than that of $V_{\text{Ga}}\text{-Si}_{\text{Ga}}$ (0.72). This is in good agreement to the experimen-

tal results. Moreover, the momentum distribution calculated for the $V_{\text{Ga}}\text{-Te}_{\text{As}}$ complex is very similar to the distribution measured in Te-doped GaAs: the intensity is increased in the momentum range $p_L = (10 - 22.5) \times 10^{-3} m_0 c$ and a crossover with the momentum distribution for $V_{\text{Ga}}\text{-Si}_{\text{Ga}}$ occurs at about $23 m_0 c$. Thus, the theoretical calculations strongly support the identification of the vacancies in GaAs:Te to be Ga-vacancy- Te_{As} -donor complexes.

Finally, we address the correlation between doping and vacancy concentration suggested by this identification. The vacancy density can be most reliably estimated from τ_{av} at high temperatures where the influence of negative ions is negligible. Using the relation $[V_{\text{Ga}}\text{-Te}_{\text{As}}] = (\tau_{\text{av}} - \tau_b) / [\mu_v \tau_b (\tau_d - \tau_b)]$ and a trapping coefficient $\mu_v = 10^{15} (T/300 \text{ K})^{-1/2} \text{ s}^{-1}$ (Refs. 9, 12, and 19), we obtain increasing vacancy densities of 0.2–0.4; 0.8–1; 3–4; and $10\text{--}20 \times 10^{17} \text{ cm}^{-3}$ with increasing doping concentration. The last value is a lower limit estimation due to saturated positron trapping. With the exception of the lowest doped sample, the ratio between vacancy and electron concentration is almost about $\frac{1}{4} \dots \frac{1}{5}$. The same relation between doping and vacancy concentration in GaAs:Te has been found earlier.¹² In that work, the carrier compensation commonly observed in GaAs:Te (Ref. 3) was interpreted as being to a large part due to dopant-vacancy complexes. The present work confirms this interpretation by the direct identification of $V_{\text{Ga}}\text{-Te}_{\text{As}}$ complexes.

In summary, we applied positron lifetime and Doppler-broadening coincidence spectroscopy to study vacancies in Te-doped GaAs. We showed that the native vacancies in GaAs:Te can directly be identified to be Ga-vacancy- Te_{As} -donor complexes. This assignment is strongly supported by theoretical calculations. No other type of vacancies could be detected for carrier densities between 5×10^{16} and $5 \times 10^{18} \text{ cm}^{-3}$, i.e., dopant-vacancy complexes rather than isolated vacancies are the dominating ones in sufficiently high n -doped, As-rich GaAs. It was demonstrated that even small differences in the positron signals can be used to obtain a direct and unambiguous identification of vacancies or vacancy complexes in GaAs thus helping to resolve former conflicting interpretations.

We thank Dr. M. Jurisch (Freiberger Compound Materials GmbH) for sample material. This work was supported by the Deutsche Forschungsgemeinschaft.

*Electronic address: gebauer@physik.uni-halle.de

¹T. Y. Tan, U. Gösele, and S. Yu, Crit. Rev. Solid State Mater. Sci. **17**, 47 (1991).

²R. C. Newman, Semicond. Sci. Technol. **9**, 1749 (1994).

³D. T. J. Hurle, J. Phys. Chem. Solids **40**, 613 (1979).

⁴G. A. Baraff and M. Schlüter, Phys. Rev. B **33**, 7346 (1986).

⁵See, e.g., S. B. Zhang and J. E. Northrup, Phys. Rev. Lett. **67**, 2339 (1991); T. Y. Tan *et al.*, Appl. Phys. A: Solids Surf. **56**, 249 (1993).

⁶D. J. Chadi, Mater. Sci. Forum **258–263**, 1321 (1997).

⁷E. W. Williams, Phys. Rev. **168**, 922 (1968).

⁸C. Domke *et al.*, Phys. Rev. B **54**, 10 288 (1996).

⁹J. Gebauer *et al.*, Phys. Rev. Lett. **78**, 3334 (1997).

¹⁰K. Saarinen *et al.*, Phys. Rev. B **44**, 10 585 (1991).

¹¹S. Fujii and S. Tanigawa, Hyperfine Interact. **79**, 719 (1993).

¹²R. Krause-Rehberg *et al.*, Phys. Rev. B **49**, 2385 (1994).

¹³M. Alatalo *et al.*, Phys. Rev. B **51**, 4176 (1995).

¹⁴M. Alatalo *et al.*, Phys. Rev. B **54**, 2397 (1996).

¹⁵P. Asoka-Kumar *et al.*, Phys. Rev. Lett. **77**, 2097 (1996); S. Zepala *et al.*, Phys. Rev. B **54**, 4722 (1996); U. Myler and P. J. Simpson, *ibid.* **56**, 14 303 (1997).

¹⁶H. Kauppinen *et al.*, J. Phys.: Condens. Matter **9**, 5495 (1997).

¹⁷T. Laine *et al.*, Phys. Rev. B **54**, R11 050 (1996).

¹⁸J. Gebauer *et al.*, Mater. Sci. Forum **258–263**, 905 (1997).

¹⁹C. Le Berre *et al.*, Phys. Rev. B **52**, 8112 (1995).

²⁰M. J. Puska, C. Corbel, and R. M. Nieminen, Phys. Rev. B **41**, 9980 (1990).

²¹B. Barbiellini *et al.*, Phys. Rev. B **53**, 16 201 (1996).